Received: 8 August 2021 | Revised: 6 January 2022 | Accepted: 23 January 2022

DOI: 10.1002/aic.17628

AIChE JOURNAL

RESEARCH ARTICLE

Reaction Engineering, Kinetics and Catalysis

New method of kinetic modeling for CO_2 absorption into blended amine systems: A case of MEA/EAE/3DEA1P trisolvent blends

Wenchao Zheng | Qinlan Luo | Sen Liu | Nan Wang | Xiao Luo | Hongxia Gao | Zhiwu Liang

Joint International Center for CO_2 Capture and Storage (iCCS), Provincial Hunan Key Laboratory for Cost-effective Utilization of Fossil Fuel Aimed at Reducing Carbon-dioxide Emissions, College of Chemistry and Chemical Engineering, The Engineering Research Center of Advanced Catalysis, Ministry of Education, Hunan University, Changsha, China

Correspondence
Xiao Luo, Hongxia Gao, and Zhiwu Liang, Joint International Center for CO_2 Capture and Storage (iCCS), Provincial Hunan Key Laboratory for Cost-effective Utilization of Fossil Fuel Aimed at Reducing Carbon-dioxide Emissions, College of Chemistry and Chemical Engineering, The Engineering Research Center of Advanced Catalysis, Ministry of Education, Hunan University, Changsha 410082, China.
Email: x_luo@hnu.edu.cn, hxgao@hnu.edu.cn, and zwliang@hnu.edu.cn

Funding information
National Natural Science Foundation of China, Grant/Award Numbers: 21776065, 22178089, 22138002

Abstract

In order to establish an accurate kinetic model for the aqueous amine blends, monoethanolamine (MEA), 2-(ethylamino) ethanol (EAE), and 3-(diethylamino)-1-propanol (3DEA1P) have been chosen as a typical CO_2 absorption trisolvents. The reaction kinetics of aqueous amine blends with carbon dioxide have been investigated first combining experiments and molecular simulations. The stopped-flow technology has been used to obtain the observed reaction rate constant of the overall reactions over the temperature range of 293 to 313 K and at different amine concentrations. A theoretical kinetic model, based on the first-principles quantum-mechanical simulations, has been put forward to interpret the reactions between CO_2 and the aqueous trisolvent amine blends systems. The proposed model, based on the zwitterion mechanism and the base-catalyzed mechanism, shows good prediction with an acceptable absolute average deviation (AAD) of 6.32%, and has been found to be satisfactory in determining the kinetics of the involved complicated reactions.

KEYWORDS
AIMD, CO_2 absorption, reaction kinetic, stopped-flow technology, trisolvent blends

1 | INTRODUCTION

Carbon dioxide (CO_2) has the greatest impact on global warming and climate change among all of the greenhouse gases (GHGs). The uncontrolled emissions of CO_2 to the atmosphere have thus become a global issue. It is generally accepted that the most convenient method for post-combustion CO_2 capture is the chemical absorption.[1,2] The ideal solvent for CO_2 absorption should have low vapor pressure, viscosity, corrosiveness and energy consumption of regeneration, and high CO_2 selective solubility, absorption rate, and CO_2 loading capacity. Alkanolamines (primary amines, secondary amines, and tertiary amines) and their properties that influence the performance of this technology have become the subjects of in-depth study in the last few decades. However, single amine solutions, with their contradictory properties of absorption efficiency and regeneration energy consumption, are limited in what they can accomplish. In order to obtain amines with both fast absorption rates and low regeneration energy consumption, the concept of mixed amine solution has become more and more attractive. The chemical reaction kinetics of CO_2 absorption in amine solutions is one of the most important parameters that impacts the reaction rate and its understanding is a prerequisite for the optimization and the industrial application of the chemical absorption process.

The growing interest in blends of amines instead of a single amine for gas absorption processes has resulted in numerous studies on the

Wenchao Zheng and Qinlan Luo contributed equally to this work.

kinetics behavior of blends of primary or secondary amines with tertiary amines. Researchers have found that mixed amines have great potential for CO_2 capture. Chakravarty et al.[3] first proposed to use blended amines to absorb acid gases. Dubois and Thomas[4] studied the absorption capacity of monoethanolamine (MEA), MDEA, and piperazine (PZ) mixtures and concluded that blended amines performed better than a single amine. Conway et al.[5] found that the CO_2 cyclic capacity of every blended amine (MEA/*N*,*N*-diethylethanolamine [DEEA], MEA/*N*,*N*-dimethylethanolamine [DMEA], and MEA/2-amino-2-methyl-1-propanol [AMP]) was significantly higher than standard MEA solutions at similar concentrations. Ali[6] found that blending AMP with either of the amines results in the improvement of the observed pseudo-first-order reaction rate constant values (k_0), which were greater than the sum of the k_0 values of the respective pure amines. The kinetics studies between CO_2 and blends of DEA/MEA were presented by Xiao et al.,[7] which indicated that the kinetics of blended amine was faster than that of a single amine as well. Jiang et al.[8] determined the kinetics of CO_2 absorption into DEEA/MEA, and DMEA/MEA using a stopped-flow apparatus and put forward a new kinetic model to describe the reaction mechanism of the tertiary/primary amines blended systems. In Jiang's model, the kinetics behavior of MEA was expressed by the termolecular mechanism instead of the zwitterion mechanism, and the base-catalyzed mechanism was employed to explain tertiary amine reactions, respectively. Nwaoha et al.[9] reported on a highly concentrated tri-solvent blend containing AMP, PZ, and MEA for CO_2 capture. Their experimental results indicated that the tri-solvent blends possessed higher cyclic capacities, higher initial desorption rates, and lower heat duties compared to MEA alone.

In 1974, Knipe et al.[10] reported a fast response conductivity amplifier for chemical kinetics which can follow the reactions with half-lives from 2 ms to several hours. Since then, various researchers have employed the stopped-flow technology with conductivity amplifier to investigate the reaction kinetics between amines and CO_2 such as Ali et al.,[11] Henni et al.,[12] Li et al.,[13]and Liu et al.[14] The stopped-flow apparatus has been proved to be a reliable experimental method for studying the kinetics of CO_2 absorption by amines, and although the gas phase dissolution process is ignored.[7,15] However, the likely elementary reactions and reaction intermediates involved in the CO_2 capture by amines are difficult to investigate using experimental methods, owning to the fast reaction rate of some elementary reactions and the instability of reaction intermediates.

A great deal of effort has been made to apply molecular simulations to understand the fundamental mechanisms underlying the CO_2 capture with aqueous alkanolamines. At first, the implicit solvent model using gas-phase or continuum-based static quantum mechanical (QM) calculation was implied to describe the reaction between CO_2 and alkanolamines.[16,17] Even some useful molecular insights into the reaction mechanisms can be provided by the implicit QM model, the calculated absorption energies were significantly lower than the experimental results.[18] This is because the microstructure of solvate/solvent cannot be taken into account by the implicit QM model, which has critically effect on the reaction between CO_2 and alkanolamines.[19] Later on, Han et al.[20] reported that the explicit solvent model including water molecules in the simulation systems via *ab initio* molecular dynamics (AIMD) simulations, which organically combine density functional theory (DFT) and molecular dynamics methods, can predict the heat of CO_2 absorption in aqueous MEA very well. Hwang et al.[21] also used AIMD to identify the likely elementary reaction steps and intermediates in MEA-CO_2-H_2O solution, demonstrating the formation of a zwitterionic intermediate during the reaction in MEA-CO_2-H_2O system. Both of Bo et al.'s[20] result and Hwang et al.'s[21] results indicated that the proton transfer of the zwitterionic intermediate was the dominant process to prompt CO_2 capture. Thus, the AIMD simulations with the explicit solvation model can be used to predict the fundamental mechanism underlying CO_2 capture by aqueous amines accurately, as the solution microstructure and dynamics and their effects are taken into consideration. Meanwhile, there are relatively few studies explore the molecular mechanism of the CO_2 absorption in amine blends,[22] especially, litter molecular understanding of how the intermolecular effects between amines or products may affect the reaction kinetics of CO_2 absorption.

MEA is the most widely used primary amine in industry, and it exhibits high absorption rate and high desorption energy consumption. Unlike MEA, 2-(ethylamino) ethanol (EAE) as a typical secondary amine, has a low corrosion rate even at higher concentrations, and it requires less energy for regeneration. Its absorption rate is higher due to the formation moderately stable carbamate.[23,24] In addition, EAE is readily obtained, which can be produced from agriculture products or residual ethanol.[25] 3-(diethylamino)-1-propanol (3DEA1P) is a tertiary amine for CO_2 capture, which exhibits a very high pKa.[26] Chowdhury et al.'s[26] experimental results including gas scrubbing absorption, vapor–liquid equilibrium (VLE), and reaction calorimetry, showed that 3DEA1P performed higher absorption rate and cyclic capacity compared with the most of other tertiary amines. Aqueous amine blends which contain MEA, EAE, and 3DEA1P as typical primary, secondary, and tertiary amines, could show better performance than both single and double amine solvent blends. However, there are still no kinetic studies for this kind of trisolvent. Therefore, this study is mainly focused on developing an accurate kinetic model through semi-empirical correlations and theoretical calculations for MEA/EAE/3DEA1P trisolvent blends. The chemical structures of used amines were detailed in Figure 1.

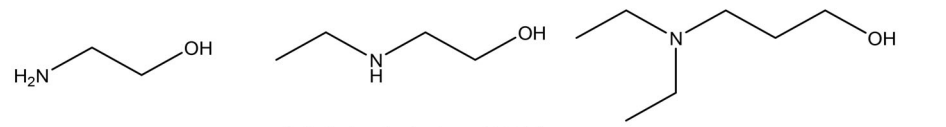

FIGURE 1 Chemical structure of used amines in this study

2 | EXPERIMENTAL SECTION

2.1 | Chemicals

3DEA1P with the purity of 97 wt% was purchased from Energy Chemical (Energy Chemical co., LTD). MEA, EAE with the purity of 99 wt% were purchased from Aladdin Reagent (Aladdin Industrial Corporation). CO_2 gas with the purity of 99.9 vol% was supplied by Changsha Rizhen Gas Co. Ltd. The deionized water was prepared by reverse osmosis ultra-pure water equipment (Model TS-RO-10 L/H, ≤0.1 μs/cm, Taoshi Water Equipment Engineering Co. Ltd.), and the deionized water was degassed by distillation and ultrasonic treatment before being used for aqueous solution preparation.

2.2 | Data collection in stopped flow apparatus

The experimental data for CO_2 absorption into MEA/EAE/3DEA1P tri-solvent blends was collected using the stopped-flow apparatus (Figure 1) as designed for directly investigating the single mixing rapid-kinetics and supplied by Hi-Tech Scientific Ltd. The stopped-flow apparatus includes four main sections: a sample handling unit, a conductivity-detection cell, an A/D converter, and a microprocessor. When the amine solution is reacted with CO_2 saturated aqueous solution, the ion concentration in the solution will change, leading to the change of the conductivity of the solution. By measuring the change in conductivity versus time with the KinetAsyst software, the apparent reaction constant can be obtained by the fitting equation: $Y = -A \cdot \exp(-k_0 t) + C$. The detailed description of this experimental method has been provided in our previous study.[27]

This technique is based on detecting the variation in electric conductivity in the solutions that occurs during the absorption reaction. The concentration of amine usually is set to be less than 1 kmol/m^3 for tertiary amines. For primary, secondary or blended amines, the selection of specific concentration range needs to be determined by preliminary experiments to ensure the reliable k_0 value.[8] In this study, the total concentrations of amine were prepared at 0.1–0.25 kmol/m^3 and ratios of primary, secondary, and tertiary amine were set to be 0:4:4, 1:3:4, 2:2:4, 3:1:4, 4:0:4.

The CO_2 saturated aqueous solutions were prepared by bubbling CO_2 through deionized water for at least half an hour in order to reach saturation and diluted to 0.015 kmol/m^3. It should be noted that the total concentration of amine in the solutions is more than five times higher than that of CO_2 to ensure that the reaction occurs under pseudo first-order conditions (k_0 is only related to the concentration of amines). All the experiments were carried out at temperatures of 293–313 K.

It is worth mentioning that the experimental technique used in this study has already been validated in our previous study.[7,28] The obtained k_0 from the stopped-flow apparatus were in good agreement with those obtained from the literature with an absolute average deviation (AAD) of 5%. Therefore, it can be inferred that the kinetics data obtained using the same stopped-flow apparatus in this study were reliable.

3 | COMPUTATIONAL METHODS

3.1 | QM calculation

AIMD simulations based on DFT were performed within the Car-Parrinello approximation using CPMD code. The generalized-gradient

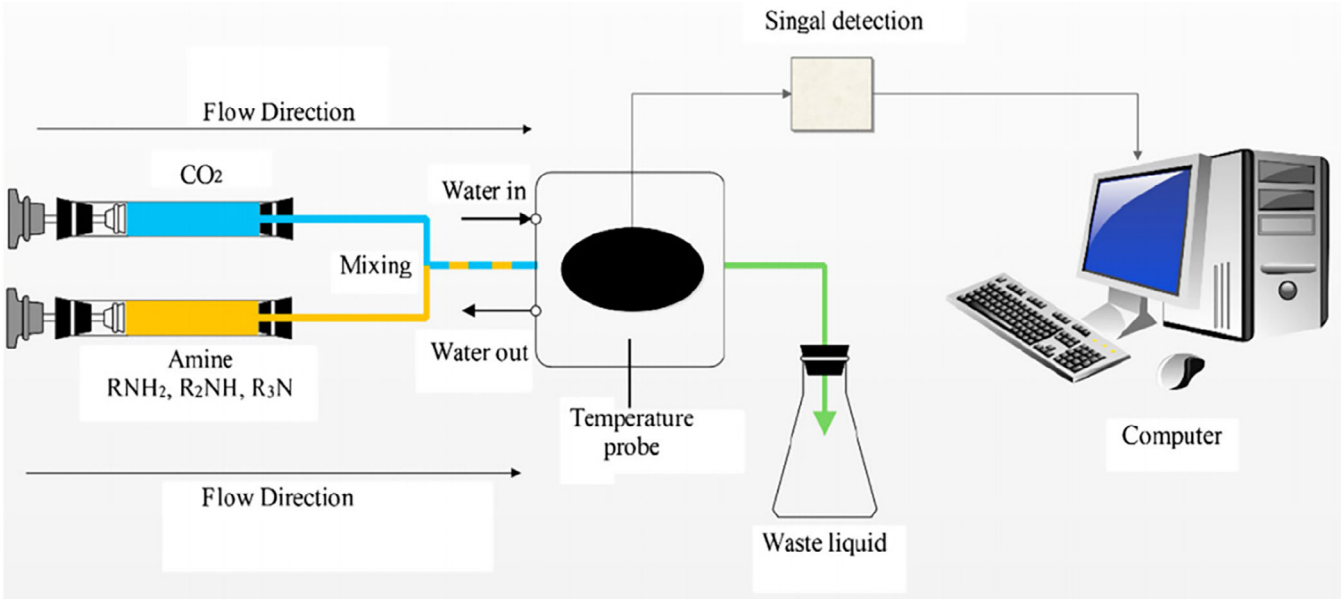

FIGURE 2 Schematic drawing of the experimental stopped-flow equipment

approximation exchange-correlation functional revised by Perdew, Burke and Ernzerhof (REVPBE)[29] was used, for the reason discussed in Hwang and Stowe's[30] study. The kinetic energy cutoff for the plane wave basis was 40 Rydberg. The timestep was set to 7 au (0.17 fs), and the fictitious electron mass was equal to 700 au. The Nosé-Hoover chain thermostat was used to control the temperature of the canonical (NVT) ensemble. The frequency for the ionic thermostat and the electron thermostat was set to 3000 and 10,000 cm^{-1}, respectively (Figures 1 and 2).

AIMD simulations were performed for six systems using a cubic box with periodic boundaries. Every system contained 30 water molecules, one amine molecule, and one zwitterion molecule in a cubic simulation box. The details of the simulation systems are shown in Table S1. For the deprotonation of MEA-zwitterion (EAE-zwitterion), three systems were built, including MEA^+COO^- + MEA aqueous system, MEA^+COO^- + EAE aqueous system, and MEA^+COO^- + 3DEA1P aqueous system (EAE^+COO^- + EAE aqueous system, EAE^+COO^- + MEA aqueous system, and EAE^+COO^- + 3DEA1P aqueous system). The relatively high reaction temperature (1000 K) and high amine concentration compared to the real experimental condition were considered to speed up the possible reactions leading to the deprotonation of zwitterions in the limited simulation time (~80 ps). The calculated density of each system was in the range of 1.007–1.037 g/cm^3. The initial structure of the systems was relaxed using the classical molecular dynamics simulations, and were then run in the microcanonical (NVE) ensemble and followed by canonical (NVT) ensemble for around 80 ps.

3.2 | Classical molecular dynamics simulation

To get the equilibrium of the simulation systems before the AIMD simulations, classical molecular dynamics simulations were performed using the Large-scale Atomic/Molecular Massively Parallel Simulator (LAMMPS) program. The modified AMBER force field was used for MEA, EAE and 3DEA1P, the SPC/E water model and the flexible EPM2 force field for CO_2 were selected. The force field parameters for MEA, EAE, 3DEA1P, water, and CO_2, including the atomic charges for these molecules, the simulation parameters and setting details were selected according to previous studies.[31,32]

4 | THEORY

4.1 | Chemical reactions

The reactions involved in MEA/EAE/3DEA1P tri-solvent blends are governed by the following chemical equations:

Ionization of water:

$$H_2O \leftrightarrow H^+ + OH^- \quad (1)$$

Bicarbonate formation from CO_2 and OH^-:

$$OH^- + CO_2 \leftrightarrow HCO_3^- \quad (2)$$

Dissociation of dissolved CO_2 through carbonic acid:

$$H_2O + CO_2 \leftrightarrow H^+ + HCO_3^- \quad (3)$$

Dissociation of bicarbonate:

$$HCO_3^- \leftrightarrow H^+ + CO_3^{2-} \quad (4)$$

Protonation of amines:

$$R_2NH/R_3N + H^+ \leftrightarrow R_2NH_2^+/R_3NH^+ \quad (5)$$

Formation of carbamate:

$$R_2NH + B + CO_2 \leftrightarrow BH^+ + R_2NCOO^- \quad (6)$$

Dissociation of protonated primary/secondary amine:

$$R_2NH_2^+ + R_3N \leftrightarrow R_2NH + R_3NH^+ \quad (7)$$

Bicarbonate formation from CO_2 and tertiary amine:

$$CO_2 + H_2O + R_3N \leftrightarrow R_3NH^+ + HCO_3^-, \quad (8)$$

where R_3N and R_2NH represent tertiary amines and primary/secondary amines, respectively. B represents amines, OH^- or H_2O.

4.2 | Kinetic model

The proposed kinetic model in this study is based on the base-catalyzed hydration mechanism[33] and zwitterion mechanism.[34,35] The base-catalyzed hydration mechanism was used to explain the reaction between CO_2 and aqueous solutions of tertiary amines where the tertiary amine does not react directly with CO_2. In this mechanism, tertiary amines act like bases to catalyze the process of CO_2 transformation to bicarbonates, as shown in Equation 8. The total reaction rate of CO_2 absorption into aqueous solution of tertiary amines can be written as follows:

$$-r_{CO_2} = k_0[CO_2] = \left\{k^B[R_3N] + k_{OH^-}[OH^-] + k_{H_2O}[H_2O]\right\}[CO_2], \quad (9)$$

where k_0 is pseudo first-order reaction rate, k^B, k_{OH^-}, k_{H_2O} are second order reaction rate constant for tertiary amine, OH^- or H_2O, respectively.

The zwitterion mechanism and the termolecular mechanism[36] are theories to explain the chemical reaction between the primary/secondary amine and CO_2. However, the termolecular mechanism assumes that three molecules collide simultaneously and effectively, which has a small probability in statistical thermodynamics. The zwitterion mechanism proposes that the reaction between CO_2 and amine

proceeds through the formation of a zwitterion as an intermediate (Equation 10):

$$R_2NH + CO_2 \xrightarrow{k_A} R_2NH^+COO^-(\text{zwitterion}) \quad (10)$$

Then the zwitterion undergoes a deprotonation process in the presence of a base to form a carbamate (Equation 11).

$$R_2NH^+COO^- + B \xrightarrow{k_B} R_2NCOO^- + BH^+, \quad (11)$$

where B represents a base (OH^-, H_2O, amines). If the deprotonation of the zwitterion is the rate-determining step ($k_B < k_A$), then the overall forward reaction rate can be expressed as follows[37,38]:

$$-r_{CO_2} = k_0[CO_2] = \left\{k_{OH^-}[OH^-] + k_{H_2O}[H_2O] + [R_2NH]\sum k^Z[B]\right\}[CO_2], \quad (12)$$

where k^Z equal to k_A multiply k_B.

In this study, the k_0 values of MEA/3DEA1P and EAE/3DEA1P for CO_2 absorption were investigated with the stopped-flow apparatus. The k_0 values of MEA and EAE for CO_2 absorption were obtained from our previous study by Liu et al.[39] The k_0 data of the four kinds of solutions were plotted with amine concentrations, as presented in Figure S1. Besides, the reaction orders of MEA, EAE, MEA/3DEA1P, EAE/3DEA1P were obtained by k_0 versus amine concentration, and exhibited in Figure 3. For the single MEA (EAE) solution, it can be assumed that the reaction between MEA (EAE) and CO_2 belong to the first-step control reaction ($k_A < k_B$), so k_0 expression can be written as $k_0 = k_2[\text{amine}]$, and the total reaction order should always be closed to 1. However, when the 3DEA1P adding to the MEA (EAE) solutions, the overall reaction order increased from 1 (1.3) to 1.2 (1.6), which means the reaction between MEA (EAE) and CO_2 becomes the second-step control reaction ($k_B < k_A$).

Thus, based on the mentioned base-catalyzed hydration, zwitterion mechanism and the discussion above, the total reaction rate of CO_2 absorption into aqueous MEA/EAE/3DEA1P trisolvent blends was composed of four parts: direct reaction of OH^- and H_2O with CO_2, absorption by 3DEA1P, absorption by MEA with different base, absorption by EAE with different base, and can be written as follows:

$$\begin{aligned}-r_{CO_2} = k_0[CO_2] = \{&k_{OH^-}[OH^-] + k_{H_2O}[H_2O] + k^B[3DEA1P] \\ &+ k^Z_{3DEA1P-MEA}[3DEA1P][MEA] + k^Z_{3DEA1P-EAE}[3DEA1P][EAE] \\ &+ k^Z_{MEA-MEA}[MEA][MEA] + k^Z_{MEA-EAE}[MEA][EAE] \\ &+ k^Z_{EAE-MEA}[EAE][MEA] + k^Z_{EAE-EAE}[EAE][EAE] \\ &+ k^Z_{H_2O-MEA}[H_2O][MEA] + k^Z_{H_2O-EAE}[H_2O][EAE] \\ &+ k^Z_{OH^--MEA}[OH^-][MEA] + k^Z_{OH^--EAE}[OH^-][EAE]\}[CO_2] \end{aligned} \quad (13)$$

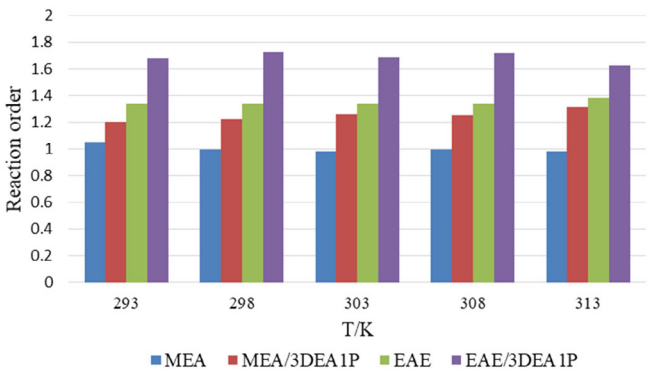

FIGURE 3 Reaction orders of MEA, EAE, MEA/3DEA1P (1:1), EAE/3DEA1P (1:1) solutions under the temperature range of 293–313 K. 3DEA1P, 3-(diethylamino)-1-propanol; EAE, 2-(ethylamino) ethanol; MEA, monoethanolamine

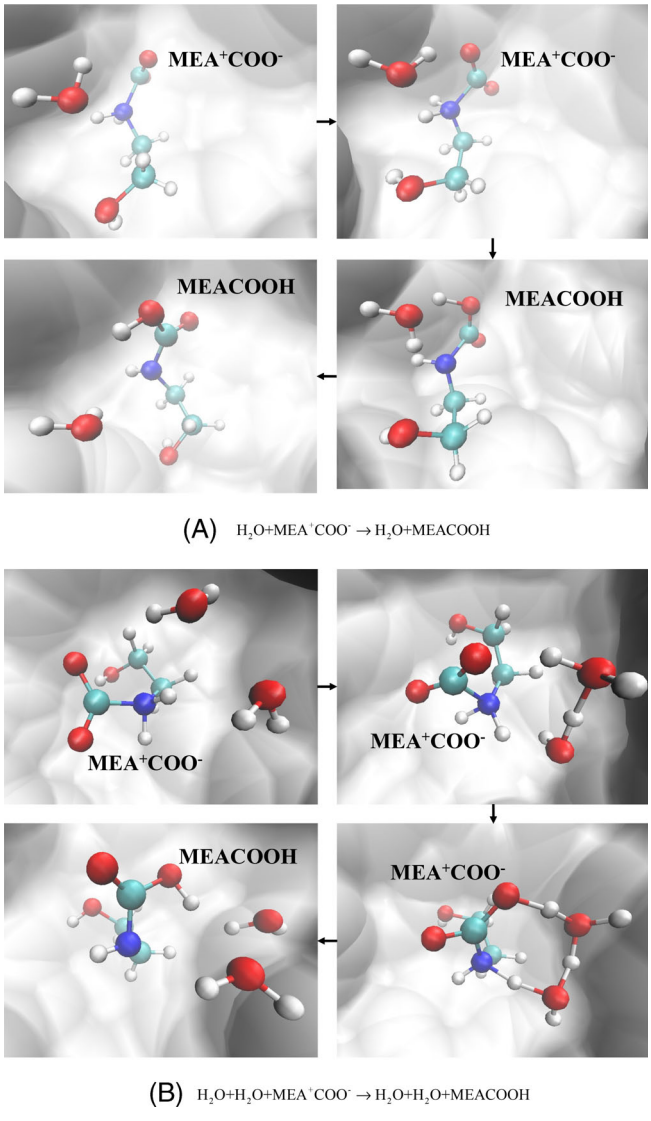

FIGURE 4 Snapshots from AIMD simulations of aqueous MEA-zwitterion at 1000 K, demonstrating the occurrence of $MEA^+COO^- \rightarrow$ MEACOOH with the help of one or two water molecules. The reactants and products are shown in Corey–Pauling–Koltun (CPK) model, other molecules in those systems are concealed. The H, C, N, and O atoms are colored in white, green, blue, and red, respectively. AIMD, *ab initio* molecular dynamics; MEA, monoethanolamine

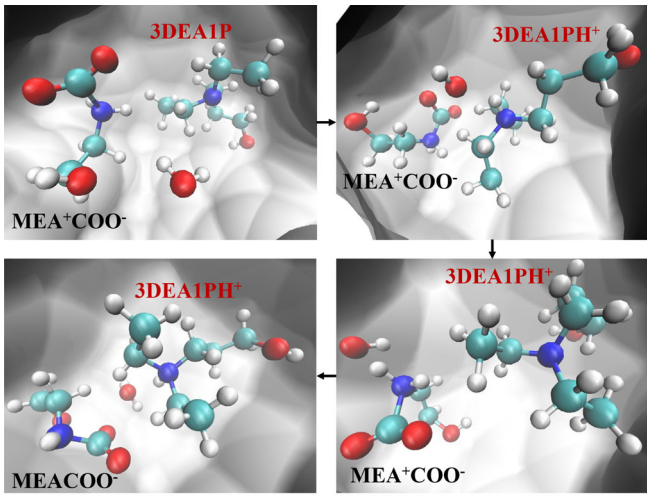

$3DEA1P+H_2O+MEA^+COO^- \rightarrow 3DEA1PH^+ + H_2O + MEACOO^-$

FIGURE 5 Snapshots from AIMD simulations of aqueous MEA^+COO^- + 3DEA1P at 1000 K, demonstrating the proton transfer from MEA^+COO^- to 3DEA1P. The reactants and products are shown in Corey–Pauling–Koltun (CPK) model, other molecules in those systems are concealed. The H, C, N, and O atoms are colored in white, green, blue, and red, respectively. 3DEA1P, 3-(diethylamino)-1-propanol; AIMD, *ab initio* molecular dynamics; MEA, monoethanolamine

TABLE 1 The pKa value comparison for 3DEA1P[44], MEA[39], and EAE[39] at different temperatures

T (K)	MEA	EAE	3DEA1P
293.15	9.64	10.11	10.27
298.15	9.51	9.98	10.16
303.15	9.33	9.80	10.04
313.15	9.07	9.54	9.82

Abbreviations: 3DEA1P, 3-(diethylamino)-1-propanol; EAE, 2-(ethylamino) ethanol; MEA, monoethanolamine.

Since the reaction rate between CO_2 and H_2O is slow, the contribution of k_{H_2O} to the total reaction rate can be neglected. The reaction between CO_2 and OH^- cannot form an extra charged particle, and thus k_{OH^-} cannot be detected in stopped-flow apparatus. Littel et al.[33] found that the concentration of OH^- ions in amine solution is very low due to the very fast reaction of CO_2 with OH^- leading to the hydroxyl ions being quickly consumed, and the effect of hydroxide ions acted as a base on the overall reaction rate can be neglected as well. Thus, Equation 13 can be further simplified as follows:

$$\begin{aligned} k_0 = {} & k^B[3DEA1P] + k^Z_{3DEA1P\text{-}MEA}[3DEA1P][MEA] \\ & + k^Z_{3DEA1P\text{-}EAE}[3DEA1P][EAE] + k^Z_{EAE/MEA}[EAE][MEA] \\ & + k^Z_{EAE\text{-}EAE}[EAE][EAE] + k^Z_{MEA\text{-}MEA}[MEA][MEA] \\ & + k^Z_{H_2O\text{-}EAE}[H_2O][EAE] + k^Z_{H_2O\text{-}MEA}[H_2O][MEA], \end{aligned} \quad (14)$$

where $k^Z_{EAE/MEA}$ was equal to $k^Z_{MEA\text{-}EAE}$ plus $k^Z_{EAE\text{-}MEA}$.

Because of the much slower kinetics for tertiary amines compared to primary/secondary amines and the small difference of the concentration of tertiary amine and primary/secondary amine, it can be approximated that the tertiary amine mainly acted as a base to participate in the deprotonating process of zwitterion (the effect of k^B on k_0 can be ignored). Thus, Equation 14 was further simplified as follows:

$$\begin{aligned} k_0 = {} & k^Z_{3DEA1P\text{-}MEA}[3DEA1P][MEA] + k^Z_{3DEA1P\text{-}EAE}[3DEA1P][EAE] \\ & + k^Z_{EAE/MEA}[EAE][MEA] + k^Z_{EAE\text{-}EAE}[EAE][EAE] + k^Z_{MEA-MEA}[MEA][MEA] \\ & + k^Z_{H_2O\text{-}EAE}[H_2O][EAE] + k^Z_{H_2O\text{-}MEA}[H_2O][MEA] \end{aligned} \quad (15)$$

For further reasonable simplification of the kinetic model, we investigated the molecular mechanisms underlying CO_2 absorption by

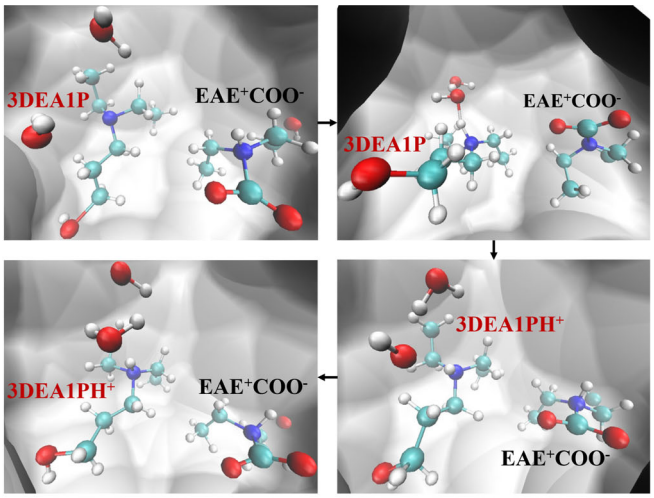

(A) $3DEA1P+H_2O+EAE^+COO^- \rightarrow 3DEA1PH^+ + OH^- + EAE^+COO^-$

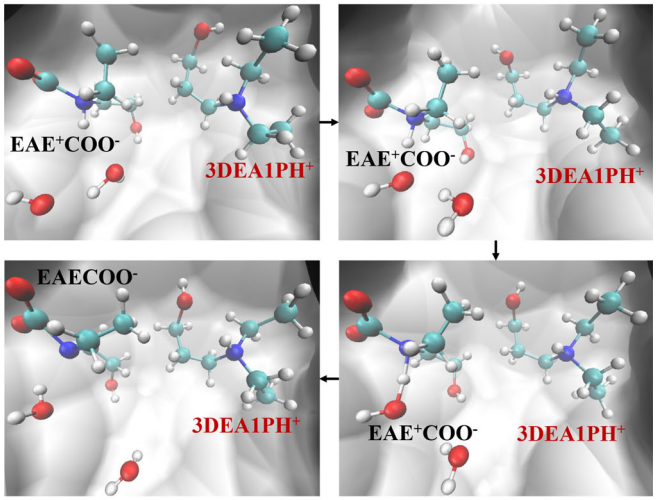

(B) $3DEA1PH^+ + H_2O + OH^- + EAE^+COO^- \rightarrow 3DEA1PH^+ + H_2O + EAECOO^-$

FIGURE 6 Snapshots from AIMD simulations of aqueous EAE-zwitterion at 1000 K, demonstrating the protonation of 3DEA1P followed by the deprotonation of EAE + COO^-. The reactants and products are shown in Corey–Pauling–Koltun (CPK) model, other molecules in those systems are concealed. The H, C, N, and O atoms are colored in white, green, blue, and red, respectively. 3DEA1P, 3-(diethylamino)-1-propanol; AIMD, *ab initio* molecular dynamics; EAE, 2-(ethylamino) ethanol

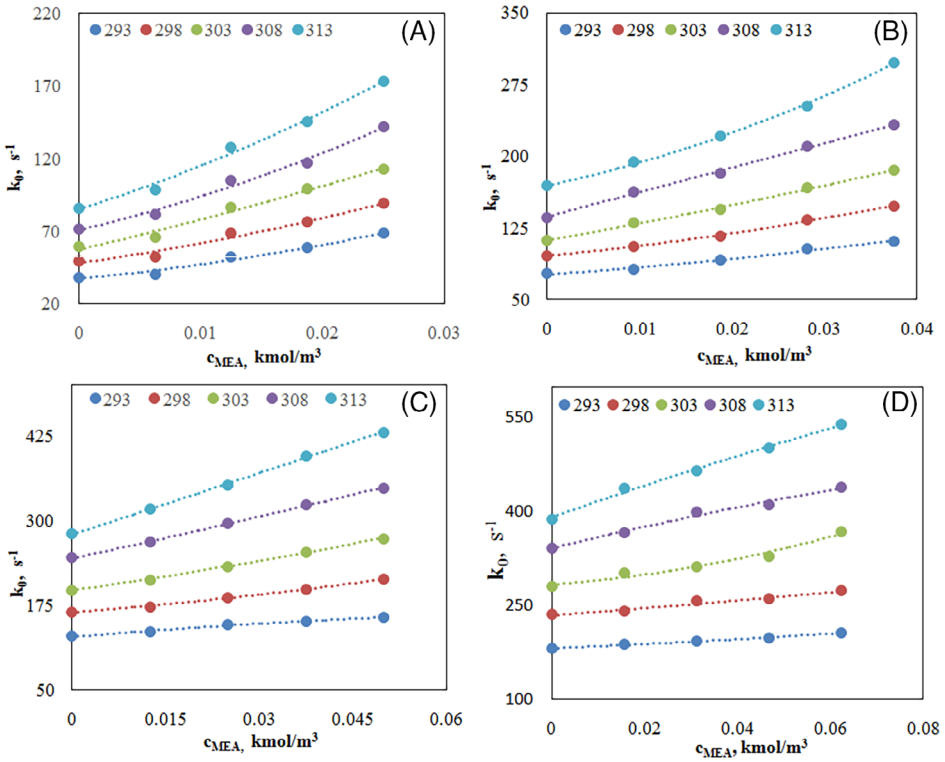

FIGURE 7 The pseudo first-order reaction rate constants of MEA/EAE/3DEA1P trisolvent blends. [The ratios of amine corresponding to MEA concentration from small to large are 0:4:4, 1:3:4, 2:2:4, 3:1:4, 4:0:4; (A), (B), (C), and (D) represent total amine concentration 0.05, 0.075, 0.1, 0.125 kmol/m^3, respectively]. 3DEA1P, 3-(diethylamino)-1-propanol; EAE, 2-(ethylamino) ethanol; MEA, monoethanolamine

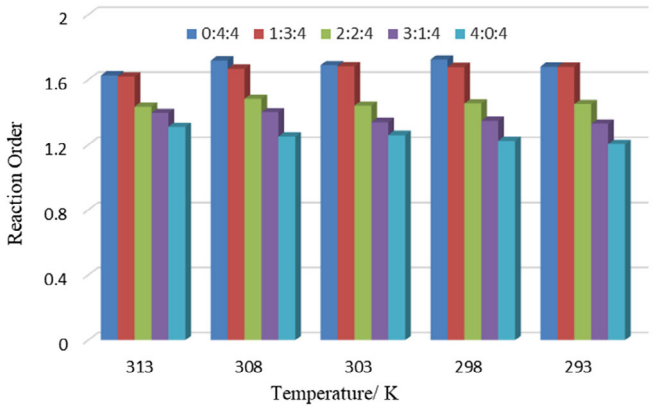

FIGURE 8 Reaction order of CO_2 absorption into MEA/EAE/3DEA1P trisolvent blends under different ratios and temperatures. 3DEA1P, 3-(diethylamino)-1-propanol; EAE, 2-(ethylamino) ethanol; MEA, monoethanolamine

aqueous MEA/EAE/3DEA1P trisolvent blends using AIMD calculations. Our experimental results pointed out that the absorption reactions between MEA and CO_2 as well as EAE and CO_2 are controlled by the second step (the deprotonation of zwitterion). Therefore, the AIMD calculations were applied to identify the likely elementary reactions and reaction intermediates during the deprotonation process of MEA-zwitterion and EAE-zwitterion.

As discussed above, in the MEA/EAE/3DEA1P trisolvent blends, many species, such as MEA, EAE, 3DEA1P, and H_2O, can play the role of the proton acceptor in the deprotonation process of MEA-zwitterion and EAE-zwitterion. To evaluate the reaction kinetic favorability of the deprotonation process, the AIMD simulations at the high reaction temperature (1000 K) were performed. Meanwhile, considering that the MEA/EAE/3DEA1P tri-solvent system has a large number of degrees of freedom, the trisolvent systems are divided into six simulation systems, as shown in Table S1. Ten independent simulations have been run for each simulation system by varying the initial distributions of molecules.

As shown in Figure 4A, the N-bond proton is transferred to the O atom of the COO^- group through the nearby water molecule, resulting in the direct formation of MEACOOH. The proton transfer can also happen through two water molecules, as shown in Figure 4B. This kind of proton transfer can be found in all aqueous MEA-zwitterion systems (MEA^+COO^- + MEA system, MEA^+COO^- + EAE, and MEA^+COO^- + 3DEA1P system). This was consistent with the simulation result from Dr. Hwang's group[21] and Kim et al.,[40] and both of them pointed out that the formation of MEACOOH by the proton transfer through two water molecules was more kinetically favorable than that through one water molecule. Our simulation results also pointed out the subsequent proton transfer from MEACOOH to other amine molecules (MEA/EAE/3DEA1P), forming protonated amine molecules ($MEAH^+$/$EAEH^+$/$3DEA1PH^+$) and $MEACOO^-$, implying that the MEACOOH can play both roles of the intermediate and the product. The phenomenon was also observed in the molecular dynamics simulations conducted by Sumon et al.[41] and Hwang et al.[21] It should be noted that the subsequent reaction following the structural diffusion (Grutthuss hopping mechanism)[42] is barrierless and happens rapidly, which means that the control step is still the deprotonation of MEA-zwitterion through the water network, accompanied by the direct formation of MEACOOH. This plays an insignificant role in the reaction kinetics compared to the direct formation of MEACOOH.

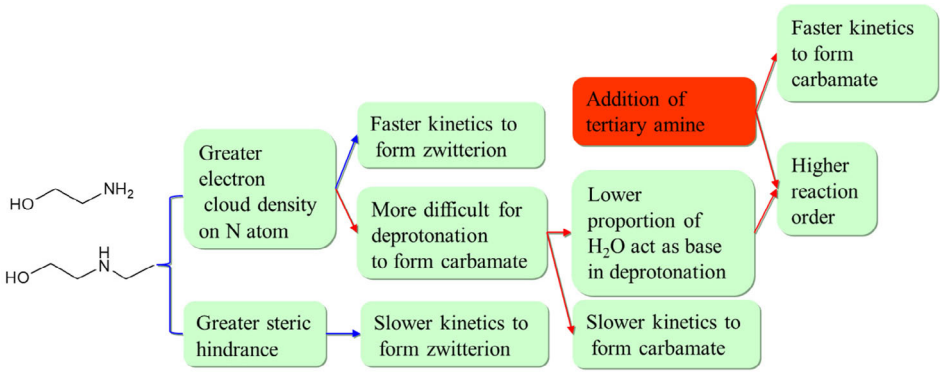

FIGURE 9 Differences between EAE and MEA. EAE, 2-(ethylamino) ethanol; MEA, monoethanolamine

Rate constant	E_a/R	E_a (kJ)	Arrhenius equation
$k^Z_{3DEA1P-MEA}$	5985.8	49.77	$k^Z_{3DEA1P-MEA} = 1.18 \times 10^{13} \times \exp(\frac{-5985.8}{T})$
$k^Z_{3DEA1P-EAE}$	3445.2	28.64	$k^Z_{3DEA1P-EAE} = 4.17 \times 10^{9} \times \exp(\frac{-3445.2}{T})$
$k^Z_{H_2O-MEA}$	3893	32.37	$k^Z_{H_2O-MEA} = 2.54 \times 10^{7} \times \exp(\frac{-3893}{T})$
$k^Z_{H_2O-EAE}$	3550.9	29.52	$k^Z_{H_2O-EAE} = 1.76 \times 10^{6} \times \exp(\frac{-3550.9}{T})$
$k^Z_{EAE-EAE}$	4920.2	40.91	$k^Z_{EAE-EAE} = 1.59 \times 10^{11} \times \exp(\frac{-4920.2}{T})$

TABLE 2 Summarized parameters for the reaction rate constants over 293–313 K

Abbreviations: 3DEA1P, 3-(diethylamino)-1-propanol; EAE, 2-(ethylamino) ethanol; MEA, monoethanolamine.

The proton transfer from MEA-zwitterion (MEA^+COO^-) to 3DEA1P through the water network can be found in most of the independent simulations of the MEA^+COO^- + 3DEA1P system, forming MEA carbamate ($MEACOO^-$) and protonated 3DEA1P ($3DEA1PH^+$). In this process, the protonation of 3DEA1P happened first, followed by the OH^- anion migration and the subsequent deprotonation of MEA^+COO^-, as shown in Figure 5. However, the proton migration from MEA^+COO^- to MEA or from MEA^+COO^- to EAE was found in only one out of 10 simulations of MEA^+COO^- + MEA system (Figure S2a) or MEA^+COO^- + EAE system (Figure S2b). This phenomenon can be explained by the basicity of the N site in MEA/EAE/3DEA1P, and specifically, compared to MEA and EAE, 3DEA1P has a higher pKa (Table 1). The lower possibility of proton migration from MEA^+COO^- to MEA is also consistent with our experimental results, which point out that the overall reaction order of MEA is 1 underlying the CO_2 capture using an aqueous low-concentration MEA solution. Therefore, the $k^Z_{3DEA1P-MEA}$ and $k^Z_{H_2O-MEA}$ in Equation 16 are very important, while $k^Z_{EAE/MEA}$ and $k^Z_{MEA-MEA}$ can be deleted. The proton transfer from EAE^+COO^- to 3DEA1P through the water network was found in the EAE^+COO^- + 3DEA1P simulation system, and after the deprotonation, the $EAECOO^-$ and $3DEA1PH^+$ were formed (Figure 6B). The AIMD simulation results showed that the protonation of 3DEA1P happened first (Figure 6A), followed by the structural diffusion of the hydroxide ion through the hydrogen bond network in water and the subsequent proton release from EAE^+COO^- to OH^-. In this deprotonation process, compared to the protonation of 3DEA1P, the barriers of the later process are insignificant if the water network allows the diffusion of the hydroxide ion.

Based on our AIMD simulation results, the Equation 15 can be simplified to the following equation:

$$k_0 = k^Z_{3DEA1P\text{-}MEA}[3DEA1P][MEA] + k^Z_{3DEA1P\text{-}EAE}[3DEA1P][EAE] + k^Z_{EAE\text{-}EAE}[EAE][EAE] + k^Z_{H_2O\text{-}EAE}[H_2O][EAE] + k^Z_{H_2O\text{-}MEA}[H_2O][MEA] \quad (16)$$

5 | RESULTS AND DISCUSSION

The pseudo first-order rate constants of CO_2 absorption into MEA/EAE/3DEA1P trisolvent blends were measured using the stopped-flow apparatus. The experiments were carried out over the concentration range of 0.05–0.125 kmol/m^3 and the temperature range of 293–313 K. The specific kinetic data was placed in Table S2. Figure 7 shows the observed pseudo-first order rate constants against the amine concentration under the temperature range of 293–313 K. It is obvious that the overall rate constant increases as the MEA concentration increases, and thus, increases as the EAE concentration decreases. Moreover, the overall rate constant was also found to increase with the increase of temperature and total amine concentration. The obtained reaction orders for each solution are exhibited in Figure 8. All the reaction orders under different temperatures decreased with the increase in the ratio of MEA/EAE, which was consistent with the proposed model.

To understand this phenomenon, we have to determine why EAE showed a higher reaction order than MEA. As shown in Figure 9, compared to MEA, EAE has an extra ethyl group on the N atom, leading to the greater steric hindrance effect and the higher electron cloud

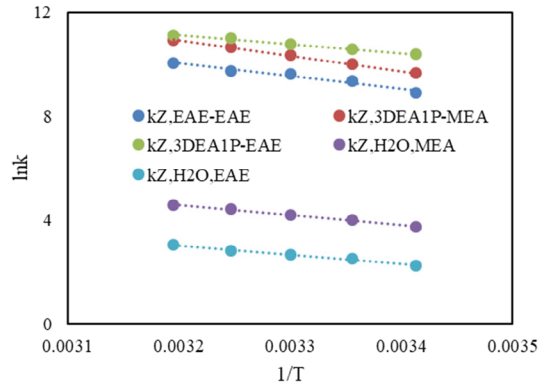

FIGURE 10 The plot of ln k against $1/T$ by using the proposed model. 3DEA1P, 3-(diethylamino)-1-propanol; EAE, 2-(ethylamino) ethanol; MEA, monoethanolamine

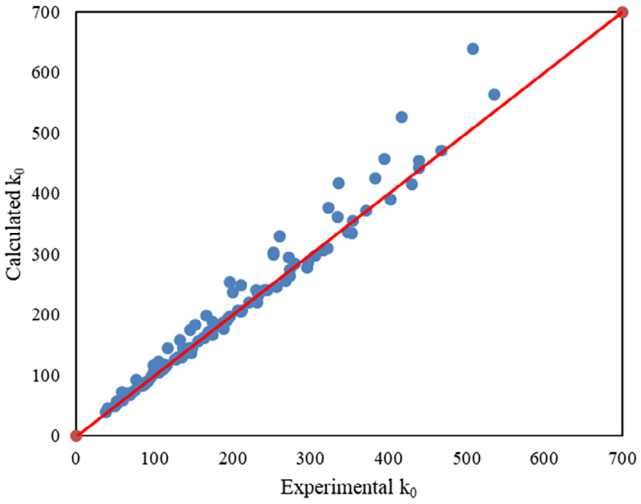

FIGURE 11 The relationship between the experimental k_0 and the calculated k_0 in trisolvent blends system by the proposed model

density (larger pKa). Higher electron cloud density will make it easier for N atoms to attack C in CO_2, and more difficult for the base to capture protons from the zwitterion. Thus, the proportion of water involved in the deprotonation process is reduced compared to the MEA, which leads to an increase of the reaction order in EAE solutions. In this blended system, we simply considered that 3DEA1P only acted as a base and MEA/EAE formed carbamate. The proportion of water involved in deprotonation process is decreased in the presence of tertiary amine. Thus, the reaction orders under different temperatures are increased with the increasing ratio of EAE.

Based on the discussion in the kinetic model section, the deprotonation step was found to be the controlling step in the formation of MEA/EAE carbamate. Due to the strong basicity of 3DEA1P, it has the ability to grab the proton in the solution, thus facilitating the proton transfer to form carbamates. Combining the study of Jiang et al.,[8] we believe that the interaction between tertiary amines and primary/secondary amines is mainly reflected in the process of deprotonation which will lead to the increase of the reaction rate constants and the raise of the overall reaction order. And, in this MEA/EAE/3DEA1P trisolvent blends system, the increase of the reaction rate caused by these interactions accounts for 14%–67% of the observed reaction rate.

5.1 | Model for trisolvent blends

The model (Equation 16 was based on the zwitterion and base-catalyzed hydration mechanism. Thus, based on the previous derivation in Section 4, $k_{0,cal}$, $k^Z_{3DEA1P\text{-}MEA}$, $k^Z_{3DEA1P\text{-}EAE}$, $k^Z_{EAE\text{-}EAE}$, $k^Z_{H_2O\text{-}EAE}$, and $k^Z_{H_2O\text{-}MEA}$ were calculated by substituting the obtained "k_0" data set into Equation 16 using nonlinear regression. Reaction rate constants are generally regarded to be a function of temperature, so the obtained data of $k_{0,cal}$, $k^Z_{3DEA1P\text{-}MEA}$, $k^Z_{3DEA1P\text{-}EAE}$, $k^Z_{EAE\text{-}EAE}$, $k^Z_{H_2O\text{-}EAE}$, and $k^Z_{H_2O\text{-}MEA}$ were fitted with the Arrhenius equation (Equation 18)[28,43] and the results are listed in Table 2. The activation energy (E_a) of $k_{0,cal}$, $k^Z_{3DEA1P\text{-}MEA}$, $k^Z_{3DEA1P\text{-}EAE}$, $k^Z_{EAE\text{-}EAE}$, $k^Z_{H_2O\text{-}EAE}$, and $k^Z_{H_2O\text{-}MEA}$ can be derived from the corresponding Arrhenius equation and are also presented in Table 2. The plot of ln(k) against $1/T$ according to Equation 18 is shown in Figure 10. It shows that the predicted Arrhenius results fit very well with the obtained data in terms of each reaction rate constant. The AAD of $k_{0,exp}$ and $k_{0,cal}$ are calculated by Equation 17

$$AAD = \frac{1}{N}\sum\left|\frac{k_{0,exp} - k_{0,cal}}{k_{0,exp}}\right| \times 100\%, \quad (17)$$

where N is the number of experimental data points.

$$k = A \times \exp\left(-\frac{E_a}{RT}\right), \quad (18)$$

where, k represents the reaction rate constant. A, E_a, and R represent the Arrhenius constant ($m^3/kmol{\cdot}s^{-1}$), activity energy (kJ/mol), and universal gas constant (8.314 J/mol·K^{-1}), respectively. A comparison of k_0 between the predicted results and the experimental results based on base-catalyzed hydration and zwitterion mechanism was made in Figure 10. An acceptable AAD of 6.32%, as shown in Figure 11, indicates that the proposed model can interpret the reaction kinetics between MEA/EAE/3DEA1P tri-solvent blends and CO_2 and predict the observe reaction rate very well. This confirms the empirical rationality of ignoring k_{OH^-}, k_{H_2O}, $k^Z_{OH^-\text{-}EAE}$, $k^Z_{OH^-\text{-}MEA}$, $k^Z_{MEA\text{-}MEA}$, k^B, $k^Z_{MEA\text{-}EAE}$, and $k^Z_{EAE\text{-}MEA}$ when building the model. Moreover, the predicted results show that the interaction between tertiary amine and primary/secondary amines is the main interaction in the studied system. The reaction rate caused by the interactions between MEA/EAE and 3DEA1P accounts for 14%–67% of the total reaction rate.

6 | CONCLUSION

The stopped-flow apparatus has been used to measure the reaction kinetics of CO_2 absorption into MEA/EAE/3DEA1P tri-solvent blends. The experimental conditions include the total amine concentration over the range of 0.05–0.125 kmol/m^3 and the temperature ranges of 293 to 313 K. The combination of base-catalyzed hydration and zwitterion mechanisms has been employed to create a new reaction kinetics model

for MEA/EAE/3DEA1P tri-solvent blends. The overall rate constant increases with increasing MEA concentration, but decreases with increasing EAE concentration. In addition, the deprotonation step in the formation of carbamate is found to be the controlling step.

The AIMD simulation results indicate that the deprotonation of MEA zwitterion can be achieved by the proton transfer through the water network (connects the N atom and O atom of MEA^+COO^-) to form MEACOOH, which is the most favorable pathway. The results also showed the feasibility of proton transfer from MEA^+COO^- or EAE^+COO^- to 3DEA1P, and in these processes, the protonation of 3DEA1P happened first, followed by the structural diffusion of the hydroxide ion through the hydrogen bond network in water and the subsequent proton release from MEA^+COO^- or EAE^+COO^- to OH^-. This phenomenon can be explained by the strong basicity of 3DEA1P, which facilitated the proton transfer and the deprotonation of MEA-zwitterion/EAE-zwitterion.

In a word, in MEA/EAE/3DEA1P trisolvent blends, the interaction between 3DEA1P and MEA/EAE are mainly reflected by the process of deprotonation, which leads to increases in the reaction rate constants and the overall reaction order. The reaction rate caused by interactions accounts for 14%–67% of the observed reaction rate. In the end, the new reaction kinetics model shows a good prediction with an acceptable AAD of 6.32%.

ACKNOWLEDGMENTS

This publication was made possible by the financial support is from the National Natural Science Foundation of China (Nos. 21776065, 22178089 and 22138002) are gratefully acknowledged. The authors especially thank Wilfred Olson for his revision of the manuscript. Helpful discussions with Gyeong S. Hwang (The University of Texas, at Austin) and assistance with calculations from Bohak Yoon (The University of Texas, at Austin) are also greatly acknowledged.

AUTHOR CONTRIBUTIONS

Wenchao Zheng: Data curation (lead); investigation (lead); methodology (lead); writing – original draft (lead). **Qinlan Luo:** Software (lead); writing – review and editing (supporting). **Sen Liu:** Investigation (supporting); methodology (supporting); software (supporting). **Nan Wang:** Investigation (supporting). **Xiao Luo:** Conceptualization (equal); supervision (lead); writing – review and editing (supporting). **Hongxia Gao:** Funding acquisition (supporting); writing – review and editing (supporting). **Zhiwu Liang:** Project administration (lead); resources (lead).

DATA AVAILABILITY STATEMENT

The data that supports the findings of this study are available in the supplementary material of this article

NOTATION

3DEA1P	3-(diethylamino)-1-propanol
A	Arrhenius constant ($m^3/kmol{\cdot}s^{-1}$)
AAD	absolute average deviation
AMP	2-amino-2-methyl-1-propanol
B	base
DEA	diethanolamine
DEEA	*N*,*N*-diethylethanolamine
DMEA	*N*,*N*-dimethylethanolamine
E_a	activity energy (kJ/mol)
EAE	2-(ethylamino) ethanol
k_0	observed pseudo first-order reaction rate constant (s^{-1})
$k_{0,cal}$	calculated pseudo first-order reaction rate constant (s^{-1})
$k_{0,exp}$	experimental observed pseudo first-order reaction rate constant (s^{-1})
k_2	second order reaction rate constant for the formation of zwitterion ($m^3/kmol{\cdot}s^{-1}$)
k_A	second order reaction rate constant for the formation of zwitterion ($m^3/kmol{\cdot}s^{-1}$)
k_B	second order reaction rate constant for deprotonation of zwitterion ($m^3/kmol{\cdot}s^{-1}$)
k_{H_2O}	second order reaction rate constant for H_2O ($m^3/kmol{\cdot}s^{-1}$)
k_{inter}	pseudo first-order reaction rate contributed by the amine interactions ($m^6/kmol^2{\cdot}s^{-1}$)
k_{OH^-}	second order reaction rate constant for OH^- ($m^3/kmol{\cdot}s^{-1}$)
k^B	second order reaction rate constant for tertiary amine ($m^3/kmol{\cdot}s^{-1}$)
$k^Z_{B-R_2NH}$	zwitterion reaction rate to form R_2NCOO^- contributed by base ($m^6/kmol^2{\cdot}s^{-1}$)
MEA	monoethanolamine
MDEA	methyldiethanolamine
PZ	piperazine
R	the universal gas constant, 8.314 $J/mol{\cdot}K^{-1}$
R_2NH	primary/second amines
R_3N	tertiary amines
T	temperature (K)

ORCID

Xiao Luo https://orcid.org/0000-0003-2201-7586
Zhiwu Liang https://orcid.org/0000-0003-1935-0759

REFERENCES

1. da Silva EF, Booth AM. Emissions from postcombustion CO_2 capture plants. *ACS Publicat*. 2013;47:659-660.
2. Rao AB, Rubin ES. A technical, economic, and environmental assessment of amine-based CO_2 capture technology for power plant greenhouse gas control. *Environ Sci Technol*. 2002;36(20):4467-4475.
3. Chakravarty T, Phukan U, Weilund R. Reaction of acid gases with mixtures of amines. *Chem Eng Prog (United States)*. 1985;81(4):32–36.
4. Dubois L, Thomas D. CO2 absorption into aqueous solutions of monoethanolamine, methyldiethanolamine, piperazine and their blends. *Chem Eng Technol*. 2009;32(5):710-718.
5. Conway W, Bruggink S, Beyad Y, et al. CO_2 absorption into aqueous amine blended solutions containing monoethanolamine (MEA), N, N-dimethylethanolamine (DMEA), N, N-diethylethanolamine (DEEA) and 2-amino-2-methyl-1-propanol (AMP) for post-combustion capture processes. *Chem Eng Sci*. 2015;126:446-454.
6. Ali SH. Kinetics of the reaction of carbon dioxide with blends of amines in aqueous media using the stopped-flow technique. *Int J Chem Kinet*. 2005;37(7):391-405.
7. Xiao S, Liu H, Gao H, et al. Kinetics and mechanism study of homogeneous reaction of CO2 and blends of diethanolamine and monoethanolamine using the stopped-flow technique. *Chem Eng J*. 2017;316:592-600.

8. Jiang W, Luo X, Gao H, et al. A comparative kinetics study of CO_2 absorption into aqueous DEEA/MEA and DMEA/MEA blended solutions. *AIChE J*. 2018;64(4):1350-1358.
9. Nwaoha C, Saiwan C, Tontiwachwuthikul P, et al. Carbon dioxide (CO2) capture: absorption-desorption capabilities of 2-amino-2-methyl-1-propanol (AMP), piperazine (PZ) and monoethanolamine (MEA) tri-solvent blends. *J Nat gas Sci Eng*. 2016;33:742-750.
10. Knipe A, McLean D, Tranter R. A fast response conductivity amplifier for chemical kinetics. *J Phys E Sci Instrum*. 1974;7(7):586-590.
11. Ali SH, Merchant SQ, Fahim MA. Reaction kinetics of some secondary alkanolamines with carbon dioxide in aqueous solutions by stopped flow technique. *Sep Purif Technol*. 2002;27(2):121-136.
12. Henni A, Li J, Tontiwachwuthikul P. Reaction kinetics of CO_2 in aqueous 1-amino-2-propanol, 3aAmino-1-propanol, and dimethylmonoethanolamine solutions in the temperature range of 298−313 K using the stopped-flow technique. *Ind Eng Chem Res*. 2008;47(7):2213-2220.
13. Li W, Xiao S, Liu S, et al. Comparative kinetics of homogeneous reaction of CO2 and unloaded/loaded amine using stopped-flow technique: a case study of MDEA solution. *Sep Purif Technol*. 2020;242:116833.
14. Liu S, Gao H, Luo X, Liang Z. Kinetics and new mechanism study of CO_2 absorption i nto water and tertiary amine solutions by stopped-flow technique. *AIChE J*. 2019;65(2):652-661.
15. Li J, Henni A, Tontiwachwuthikul P. Reaction kinetics of CO_2 in aqueous ethylenediamine, ethyl ethanolamine, and diethyl monoethanolamine solutions in the temperature range of 298−313 K, using the stopped-flow technique. *Ind Eng Chem Res*. 2007;46(13):4426-4434.
16. Da Silva EF, Svendsen HF. Ab initio study of the reaction of carbamate formation from CO_2 and alkanolamines. *Ind Eng Chem Res*. 2004;43(13):3413-3418.
17. Arstad B, Blom R, Swang O. CO_2 absorption in aqueous solutions of alkanolamines: mechanistic insight from quantum chemical calculations. *J Phys Chem A*. 2007;111(7):1222-1228.
18. Shim JG, Kim JH, Jhon YH, Kim J, Cho KH. DFT calculations on the role of base in the reaction between CO_2 and monoethanolamine. *Ind Eng Chem Res*. 2009;48(4):2172-2178.
19. Da Silva EF, Svendsen HF. Study of the carbamate stability of amines using ab initio methods and free-energy perturbations. *Ind Eng Chem Res*. 2006;45(8):2497-2504.
20. Han B, Zhou C, Wu J, Tempel DJ, Cheng H. Understanding CO $_2$ capture mechanisms in aqueous monoethanolamine via first principles simulations. *J Phys Chem Letters*. 2010;2(6):522-526.
21. Hwang GS, Stowe HM, Paek E, Manogaran D. Reaction mechanisms of aqueous monoethanolamine with carbon dioxide: a combined quantum chemical and molecular dynamics study. *Phys Chem Chem Phys*. 2015;17(2):831-839.
22. Shi H, Fu J, Wu Q, Huang M, Jiang L, Cui M, Idem R, Tontiwachwuthikul P. Studies of the coordination effect of DEA-MEA blended amines (within 1+4 to 2+3 M) under heterogeneous catalysis by means of absorption and desorption parameters. *Separation and Purification Technology*. 2020;236:116179.
23. Mimura T, Suda T, Iwaki I, Honda A, Kumazawa H. Kinetics of reaction between carbon dioxide and sterically hindered amines for carbon dioxide recovery from power plant flue gases. *Chem Eng Commun*. 1998;170(1):245-260.
24. Suda T, Iwaki T, Mimura T. Facile determination of dissolved species in CO_2-amine-H_2O system by NMR spectroscopy. *Chem Lett*. 1996;25(9):777-778.
25. Sutar PN, Jha A, Vaidya PD, Kenig EY. Secondary amines for CO_2 capture: a kinetic investigation using N-ethylmonoethanolamine. *Chem Eng J*. 2012;207:718-724.
26. Chowdhury FA, Yamada H, Higashii T, Goto K, Onoda M. CO_2 capture by tertiary amine absorbents: a performance comparison study. *Ind Eng Chem Res*. 2013;52(24):8323-8331.
27. Zheng W, Jiang W, Zhang R, Luo X, Liang Z. Study of equilibrium solubility, NMR analysis, and reaction kinetics of CO_2 absorption into aqueous N 1, N 2-dimethylethane-1, 2-diamine solutions. *Energy Fuel*. 2019;34(1):672-682.
28. Liu H, Liang Z, Sema T, et al. Kinetics of CO_2 absorption into a novel 1-diethylamino-2-propanol solvent using stopped-flow technique. *AIChE J*. 2014;60(10):3502-3510.
29. Zhang Y, Yang W. Comment on "generalized gradient approximation made simple". *Phys Rev Lett*. 1998;80(4):890.
30. Stowe HM, Hwang GS. Molecular insights into the enhanced rate of CO_2 absorption to produce bicarbonate in aqueous 2-amino-2-methyl-1-propanol. *Phys Chem Chem Phys*. 2017;19(47):32116-32124.
31. Stowe HM, Vilčiauskas L, Paek E, Hwang GS. On the origin of preferred bicarbonate production from carbon dioxide (CO_2) capture in aqueous 2-amino-2-methyl-1-propanol (AMP). *Phys Chem Chem Phys*. 2015;17(43):29184-29192.
32. Stowe HM, Paek E, Hwang GS. First-principles assessment of CO_2 capture mechanisms in aqueous piperazine solution. *Phys Chem Chem Phys*. 2016;18(36):25296-25307.
33. Littel R, Van Swaaij WPM, Versteeg G. Kinetics of carbon dioxide with tertiary amines in aqueous solution. *AIChE J*. 1990;36(11):1633-1640.
34. Caplow M. Kinetics of carbamate formation and breakdown. *J Am Chem Soc*. 1968;90(24):6795-6803.
35. Danckwerts P. The reaction of CO_2 with ethanolamines. *Chem Eng Sci*. 1979;34(4):443-446.
36. Hagewiesche DP, Ashour SS, Al-Ghawas HA, Sandall OC. Absorption of carbon dioxide into aqueous blends of monoethanolamine and N-methyldiethanolamine. *Chem Eng Sci*. 1995;50(7):1071-1079.
37. Luo X, Hartono A, Hussain S, Svendsen HF. Mass transfer and kinetics of carbon dioxide absorption into loaded aqueous monoethanolamine solutions. *Chem Eng Sci*. 2015;123:57-69.
38. Aboudheir A, Tontiwachwuthikul P, Chakma A, Idem R. Kinetics of the reactive absorption of carbon dioxide in high CO_2-loaded, concentrated aqueous monoethanolamine solutions. *Chem Eng Sci*. 2003;58(23–24):5195-5210.
39. Liu S, Ling H, Gao H, et al. Kinetics and new Brnsted correlations study of CO_2 absorption into primary and secondary alkanolamine with and without steric-hindrance - ScienceDirect. *Separat Purif Technol*. 2020;233:115998.
40. Kim S, Shi H, Lee JY. CO_2 absorption mechanism in amine solvents and enhancement of CO_2 capture capability in blended amine solvent. *Int J Greenhouse Gas Control*. 2016;45:181-188.
41. Sumon KZ, Henni A, East A. Molecular dynamics simulations of proposed intermediates in the CO_2 + aqueous amine reaction. *J Phys Chem Lett*. 2014;5(7):1151-1156.
42. Castañeda S, Ribadeneira R. Description of hydroxide ion structural diffusion in a quaternized SEBS anion exchange membrane using ab initio molecular dynamics. *J Phys Chem C*. 2020;124(18):9834-9851.
43. Liu B, Luo X, Liang Z, et al. The development of kinetics model for CO_2 absorption into tertiary amines containing carbonic anhydrase. *AIChE J*. 2017;63:4933-4943.
44. Liu S, Ling H, Gao H, Tontiwachwuthikul P, Liang Z. Better choice of tertiary alkanolamines for postcombustion CO_2 capture: structure with linear alkanol chain instead of branched. *Industrial & Engineering Chemistry Research*. 2019;58(33):15344–15352.

SUPPORTING INFORMATION

Additional supporting information may be found in the online version of the article at the publisher's website.

How to cite this article: Zheng W, Luo Q, Liu S, et al. New method of kinetic modeling for CO_2 absorption into blended amine systems: A case of MEA/EAE/3DEA1P trisolvent blends. *AIChE J*. 2022;68(6):e17628. doi:10.1002/aic.17628